

N72-12443

**NASA TECHNICAL
MEMORANDUM**

NASA TM X-67969

NASA TM X-67969

**CASE FILE
COPY**

**TURBULENCE MEASUREMENTS USING THE LASER
DOPPLER VELOCIMETER**

by John W. Dunning, Jr.
Lewis Research Center
Cleveland, Ohio

and

Neil S. Berman
Arizona State University
Tempe, Arizona

TECHNICAL PAPER presented at
Symposium on Turbulence in Liquids sponsored
by the Department of Chemical Engineering
of the University of Missouri
Rolla, Missouri, October 4-6, 1971

TURBULENCE MEASUREMENTS USING THE LASER DOPPLER VELOCIMETER

by

John W. Dunning, Jr.
NASA Lewis Research Center
Cleveland, Ohio

and

Neil S. Berman
Arizona State University
Tempe, Arizona

E-6683

Although the laser Doppler velocimeter has been used for turbulence measurements in the past (1,2), no set of measurements in practical turbulent flows has been available to evaluate the instrument. In this work we examine in detail the photomultiplier signal representing the axial velocity of water within a glass pipe. We show that with proper analysis of the photomultiplier signal, the turbulent information that can be obtained in liquid flows is equivalent to recent hot film studies. In shear flows the signal from the laser Doppler velocimeter contains additional information which may be related to the average shear.

EXPERIMENTAL APPARATUS

The laser Doppler velocimeter located at the NASA Lewis Research Center is a one dimensional instrument with an optical arrangement of the Goldstein-Kreid type (3). A scattering angle of approximately 9.9 degrees as measured in water was used along with a Bragg tank which gave a static frequency shift of 30 MHz (zero velocity equals 30 MHz). The laser was a Spectra Physics Model 125. The frequency spectrum of the photomultiplier signal could be directly displayed on a Hewlett-Packard 8553 spectrum analyzer. Alternately the photomultiplier signal could be mixed with a signal from a local oscillator and the difference sent to an FM demodulator.

Two different demodulators were used, a fixed center frequency phase lock loop and a tunable discriminator which utilized pulse averaging demodulation.

The flow system was a recirculating water unit with an automatic level control on the head tank. The level in the head tank could be controlled to within ± 1.5 mm. This is equivalent to a 0.1% control of total head. Glass pipes 1.9 cm, 2.54 cm, and 5.08 cm in diameter were used in the test section and measurements were made approximately 300 cm downstream of an entrance section. Water containing a small amount of 0.5 micron polystyrene spheres was used in the system.

SPECTRUM ANALYZER RESULTS

We consider first the spectrum analyzer display of the voltage or power in the signal as a function of frequency. This signal is the laser Doppler velocimeter frequency shift and is proportional to axial velocity. Figure 1 shows spectrum analyzer traces for turbulent flow using an average of several sweeps and a single sweep. Parameters for this figure are sweep width 10 kHz/division, band width 300 Hz, sweep time 0.2 seconds per sweep. The data were obtained with a 150 mm lens focusing the laser beam at the centerline of the 5.08 cm diameter pipe with a local mean velocity of 24.5 cm/sec (local $N_{Re} = 14\ 000$). Note that the single sweep has some width corresponding to the signal broadening due to the finite sample volume as discussed by Edwards et al. (4). It can be seen that the representation of turbulence requires long time averaging and some interpretation. The noise level is also significant. In laminar flow, similar spectrum analyzer traces in Figure 2 show no difference in signal broadening for multiple and single traces. Here the velocity is

5.25 cm/sec with the same pipe, optics and spectrum analyzer bandwidth. The other parameters are sweep width 2 kHz/division and sweep time 0.005 ms/division. The signal broadening of approximately 600 Hz at the one-half power point is considerably less than the 7500 Hz for turbulent flow. The 600 Hz can be calculated from the dimensions of the scattering volume and represents the finite volume broadening. In Figure 1 the finite volume broadening would be 2500 Hz, considerably less than the observed broadening which contains the turbulent fluctuations.

To obtain the turbulence intensity from the pictures of the spectrum analyzer traces, the finite volume broadening and noise must be subtracted. The analysis must also recognize that the white area on Figure 1 is bordered by the peaks of the single traces. The corrections are possible if Gaussian distributions are assumed but may be weighted by recent events on the screen. To avoid this problem the voltage or heights of the trace at discrete frequencies can be averaged over a suitable length of time. Figure 3 shows the result of a one second average at each point plotted as normalized power versus frequency. The solid line is a least squares fit of a Gaussian plus a linear function to the data. For this experiment at the centerline of a 2.54 cm diameter pipe, the local mean velocity was 292 cm/sec corresponding to a local Reynolds number of 86 000. The turbulence intensity was 3.1%. Using the analysis of Lumley and Panofsky (5), the "probable error" in the second moment for the one second average is $\pm 20\%$ and the "probable error" in the fourth moment is $\pm 46\%$. The type of curve given in Figure 3 is equivalent to a velocity probability versus velocity curve and the error analyses of Lumley and Panofsky should hold.

In shear flows especially near the wall of a pipe, the probability distribution becomes wider. Figure 4 shows multiple sweeps and a single sweep on the spectrum analyzer for this case. Here the sweep width is 20 kHz/division, the bandwidth is 1.0 kHz and the sweep time is 0.02 sec/division. The location in the 5.08 cm diameter pipe is at $r/R = 0.92$ and the local mean velocity is 23.3 cm/sec. The single sweep is exactly the same as before with its width determined by the finite sample volume. The long time average, however, contains turbulence broadening, and an additional broadening due to velocity gradients in the radial direction. If this signal is treated the same as the previous one using a one second average per point, Figure 5 is obtained. The solid line represents the Gaussian plus linear fit. Obviously much longer averaging times are needed.

DEMODULATED SIGNAL

Spectrum analyzer averages or traces do not give information on the time variations of the turbulence. Therefore such information as the autocorrelation or the power density spectrum is unavailable from spectrum analyzer measurements. The probability density is available but is clouded by noise when a spectrum analyzer is used. FM demodulation techniques can be used to bypass the noise problem inherent in the spectrum analyzer and to yield a signal which can be processed to obtain the statistical data mentioned above. Basically we want to convert the frequency variations in the Doppler signal into voltage variations so that we may conveniently analyze the information content of the fluctuations. Figure 6 shows schematically the method used in this work. Optical heterodyning of the scattered and reference beams at the photomultiplier tube

gives a frequency shift, Δf , proportional to the instantaneous velocity, $\underline{u} + \underline{u}'$. This fluctuating frequency is heterodyned with a constant frequency, f , to move the signal to $|f - \Delta f|$, the center frequency of the FM demodulator. The demodulated output, after a low pass filter, is a voltage v proportional to the fluctuating velocity \underline{u}' . This voltage was recorded on an FM tape recorder. At a later time the tape was played back into an analog to digital conversion facility which digitized the fluctuating voltage signal and made a digital tape. In the analog to digital conversion, 13 bits were available to convert -10 to +10 volts to digital numbers from 0 to 8192. The digital tapes were processed on an IBM 360/67 computer to obtain power spectra, autocorrelations, and probability distributions.

As a test of the noise level of the electronics and the roll-off of the low pass filter a signal, frequency modulated by white noise, was made the input to the FM demodulator and processed as shown in Figure 6. The low pass filter was set at 500 Hz, and the digitizing rate at 8000 per second. The power spectrum is shown in Figure 7. The tape and digital noise level was extremely low at $2 \times 10^{-2} \text{ mv}^2/\text{Hz}$.

A typical power spectral density at the centerline is shown in Figure 8 and is compared to the data of Resch (6) at the same Reynolds number. The local mean velocity was 54 cm/sec in the 2.54 cm pipe giving a local Reynolds number of 15 000 and a turbulence intensity of 3.9%. For purposes of digital analysis, the data was divided into two regions:

- 1) below 100 Hz was digitized at 1000 pts/sec for 16 seconds; 2) above 100 Hz was digitized at 8000 pts/sec for 2 seconds. The "probable errors" are greatest at the lower end of each frequency range and are estimated

to be 21% at 4 Hz and 12% at 100 Hz. The points shown were obtained by using the Fortran program "Rapsody" written by Brumbach (7). A Parzen filter was used to smooth the raw spectra. The interesting detail about this spectrum is the noise level appearing at 400 Hz. This is the finite volume effect. The spectrum of the finite volume broadening appears flat or perhaps slightly decreasing as frequency increases. If this level is subtracted from the spectrum, the turbulent spectrum falls on the values obtained by Resch. Similar results have been found by George and Lumley (8). The finite volume effect can also be seen in oscilloscope traces of the demodulated signal. In Figure 9 the top trace is the unfiltered signal including the high frequency finite volume effect. From the power spectrum for this experiment we can select 300 Hz as the frequency beyond which turbulence is negligible. When we use a 300 Hz low pass filter, we obtain the lower curve which represents the turbulence. It would be necessary to use such a filter to get meaningful autocorrelation and probability results for any turbulent data obtained from a laser Doppler velocimeter.

From a laminar flow analysis of the laser Doppler velocimeter (4), the standard deviation of the finite volume broadening can be used to determine the size of the sample volume in the axial direction and in the radial direction, σ_x and σ_z , respectively. For spot size we use the definition of Edwards, et al. (4). These spot sizes, which are only functions of the total optical system, are given for three different lenses in Table I. In turbulent flow (assuming Gaussian signals), for long time averages, the variance of the spectrum analyzer spectrum is approximately the sum of the variances of the turbulence broadening, the

finite volume broadening, and the velocity gradient broadening. The analysis of the demodulated signal is more complicated. Some results were given by Lumley, et al. (1) previously. We would predict, regardless of the absolute location of the finite volume broadening in the power spectral density, that the turbulent spectrum at low frequencies would be independent of the finite volume broadening. Further, the height of the spectrum of the finite volume broadening at zero frequency would be proportional to the mean velocity in the volume and the reciprocal of the axial dimension of the sample volume if no velocity gradients are present. If the finite volume broadening spectrum is flat at least as far out in frequency as the intersection with the turbulent curve, we can use the level at the intersection as representing the level at zero frequency.

To study the effect of sample volume size or lens focal length on the finite volume broadening spectra, we have performed several experiments whose results are given in Figures 10, 11, and 12. Figure 10 represents the tail of the spectrum from the flow in the 2.54 cm pipe at a mean local velocity at the centerline of 54 cm/sec. The local Reynolds number is 15 000 and the turbulence intensity is 3.9%. We have converted the vertical scale to units of Hz (deviation from the mean) squared per Hz frequency to compare the result to that predicted by George and Lumley (8). Although the height of the two flat portions of the curves, representing the finite volume broadening, varies correctly with the scattering volume size, the levels predicted by George and Lumley given by the marks on the right are high. The digitizing rate for this experiment was 8000 per sec and the low pass filter was set at 2500 Hz. An EMR Model

4140 tunable discriminator with a 5 pole Bessel low pass output filter was used with a center frequency of 200 kHz and a percent bandedge of $\pm 30\%$. The sample time was 2 seconds. The waves in the spectrum are characteristic of the filter.

A similar experiment was run using a lower Reynolds number, 6000, and an EMR model 167 phase lock loop demodulator. The center frequency was 185 kHz and the bandedge deviation was ± 16.5 kHz. An external 4 pole Butterworth bandpass filter (0.2-2000 Hz) was used before taping and a 6 pole Bessel low pass filter set at 2000 Hz was installed before the digitizer to obtain the data shown in Figure 11. For the two lenses used in Figure 10 the results are the same. Here at the centerline of a 1.9 cm pipe the velocity was 28 cm/sec and the turbulence intensity 3.9%. The finite volume broadening is low enough so that some drop off from a flat spectrum can be seen for the larger focal length lens and the spectrum could be interpreted to be higher than an extrapolation from the previous curve thus agreeing with the prediction of George and Lumley. Therefore, the 50 cm focal length lens was used and its spectrum is higher than predicted. The marks on the right side again are the values of George and Lumley. Clearly there is some other effect contributing. Since the effect increases with focal length, we suspect the velocity gradients across the sample volume in the radial direction.

Using the same apparatus and procedure as in Figure 11, we measured the spectrum at r/R approximately 0.8 where the velocity gradient for this low Reynolds number is quite high. The local mean velocity was 26 cm/sec, almost the same as the previous centerline run, but the turbulence intensity was doubled and equal to about 7.7%. In Figure 12 the

tails of the spectra for the three lenses are compared. The lines on the left are the centerline levels adjusted for the mean velocity difference. Note that the 3.75 cm focal length lens which gives a very small sample volume in all directions gives the same noise level as at the centerline, but the others are much higher. In fact the 50 cm focal length lens giving the largest radial dimension leads to a noise level considerably higher than that predicted for finite volume broadening alone. We conclude that the additional effect is due to velocity gradients. Although, again, the complete spectrum must be known before a proper analysis of the turbulence can be made, the additional information is related to the shear in the sample volume. George and Lumley predict that two point correlation experiments can be used to eliminate the finite volume broadening since when the volumes do not overlap the signals will not correlate. This may not be true for the additional source of broadening. Clearly there is more work to be done in use of the laser Doppler velocimeter in shear fields.

COMPARISON OF PROBABILITY DISTRIBUTIONS

FM demodulation and subsequent removal of the finite volume broadening leads to a remarkably noise free signal that can be used to obtain velocity probability distributions. Such a result can be compared to the spectrum analyzer trace. In Figure 13 we show the probability distribution at the centerline of the 2.54 cm pipe for the same run as Figure 3. The local Reynolds number was 86 000, mean local velocity, 292 cm/sec, and turbulence intensity 3.15%. For the digital analysis we used a rate of 1000 points/sec for 21.648 sec. Based on a significant frequency of 10 Hz, the "probable error" is 4% in the second moment and 10% for the fourth moment. The skewness of -0.516 and flatness of 3.23 agree with

recent data of Bose (9). This distribution appears on a semi-log plot to be decidedly non-Gaussian, however, the departure from Gaussian behavior within the first two standard deviations is small. When we compare Figures 3 and 13 on the same scales, Figure 14 is obtained. Here the solid line is the digital analysis and the dots correspond to the spectrum analyzer trace with the linear noise trends removed. The two curves can be made to coincide by subtracting the additional noise in the spectrum analyzer trace.

This noise appears to be a function of signal and is shaped by a band pass filter which follows the photomultiplier in the apparatus used in this study.

CONCLUSIONS

As a final demonstration of the ability of the laser Doppler velocimeter we show the complete corrected spectra in Figure 15 for the three Reynolds numbers that have been used in this work. The form is similar to that given by Resch and the area under the curve is normalized to 1. This graph shows that the data obtainable in liquid flows where the turbulence intensity is as large as that obtainable at pipe centerlines in fully developed flow is comparable to hot film work. We have also shown that additional information is available from the LDV signals in shear flows.

This paper has emphasized the correction of the unique pitfalls in the analysis of laser Doppler data. Without subtraction of the finite volume and other broadening, use of correct low pass filters, and sufficient averaging time, the data can be easily misinterpreted. We are confident that the laser Doppler technique is a valuable aid to the study

of turbulence and can provide low frequency turbulent information unobtainable by any other means.

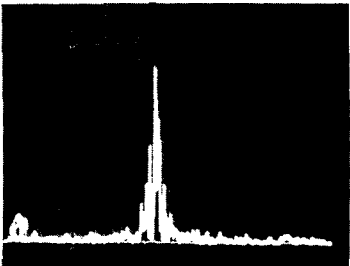
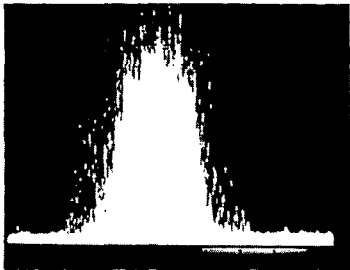
REFERENCES

1. J. L. Lumley, W. K. George and Y. Kobashi, "The influence of ambiguity and noise on the measurement of turbulent spectra by Doppler scattering," in Turbulence Measurements in Liquids, ed. by G. K. Patterson and J. C. Zakin, Department of Chemical Engineering, University of Missouri-Rolla, 1971.
2. R. J. Goldstein, R. J. Adrian and D. K. Kreid, "Turbulent and transition pipe flow of dilute aqueous polymer solutions," I & EC Fundamentals, 8, 498 (1969).
3. R. J. Goldstein, and D. K. Kreid, J. Appl. Mech, "Measurement of Laminar Flow Development in a Square Duct Using a Laser Doppler Flowmeter," 34-E, 813 (1967).
4. R. V. Edwards, John C. Angus, M. J. French and J. W. Dunning, "Spectral analysis of the signal from the laser Doppler flowmeter: Time Independent Systems," J. Appl. Phys., 42, 837 (1971).
5. J. L. Lumley and H. A. Panofsky, "The structure of atmospheric turbulence," Interscience, New York, 1964.
6. F. Resch and M. Coantic, "Etude sur le fil chaud et le film chaud dans l'eau," La Houille Blanch 1969, 151 (1969).
7. R. P. Brumback, "Digital computer routines for power spectral analysis," AC Electronics, Santa Barbara, California, July 1968.
8. W. K. George and J. L. Lumley, "Limitations on the measurement of turbulence using a laser Doppler velocimeter," Preprint 1345 ASCE National Water Resources Engineering Meeting, Phoenix, Arizona, January, 1971.
9. B. Bose, "Some measurement in pipe flow," AIAA Journal, 9, 1405 (1971).

Table I
CHARACTERISTICS OF LENSES FROM LAMINAR FLOW

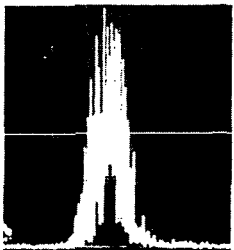
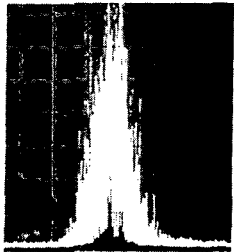
NOMINAL FOCAL LENGTH, CM	σ_x , μM	σ_z , μM
3.75	3	15
15	7	140
50	20	400

CS-60125



CS-60112

Figure 1



CS-60113

Figure 2

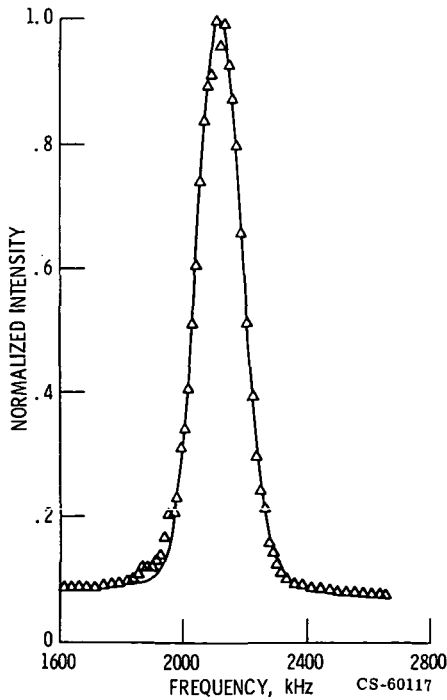
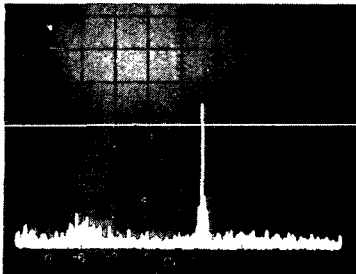
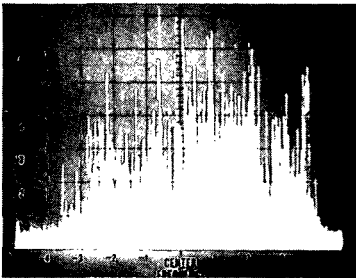


Figure 3

CS-60117



CS-60111

Figure 4

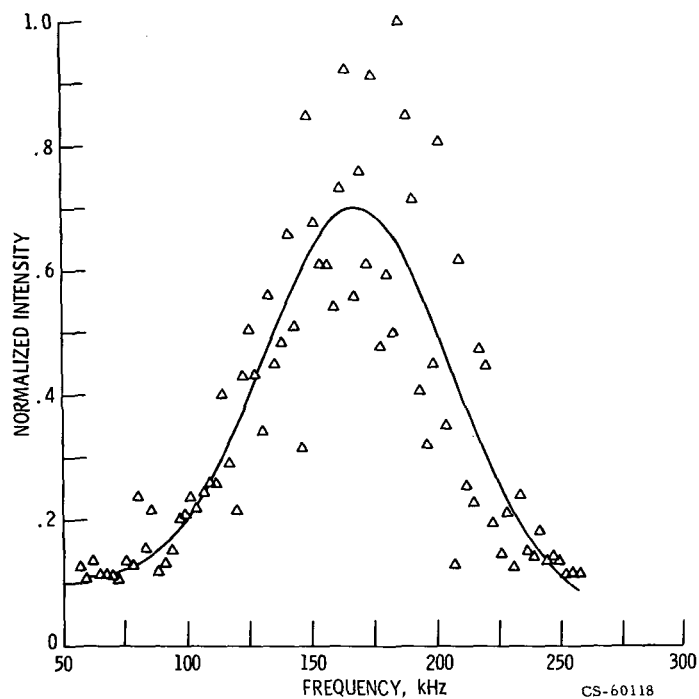


Figure 5

$$\Delta f = \frac{2\eta(\underline{u} + \underline{u}')}{\lambda} \sin \frac{\theta}{2}$$

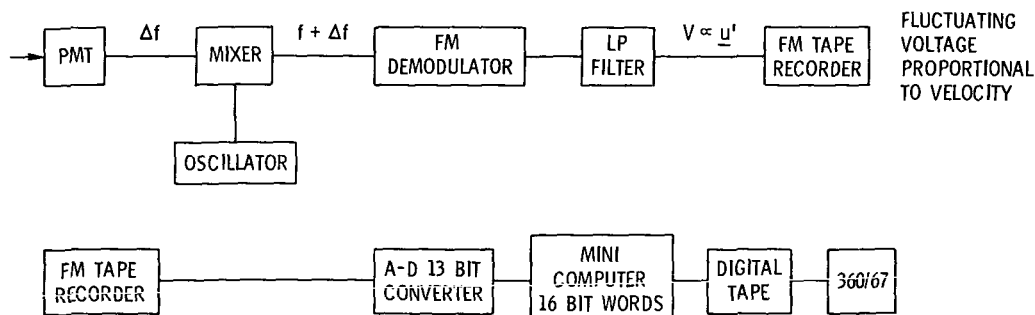


Figure 6

CS-60116

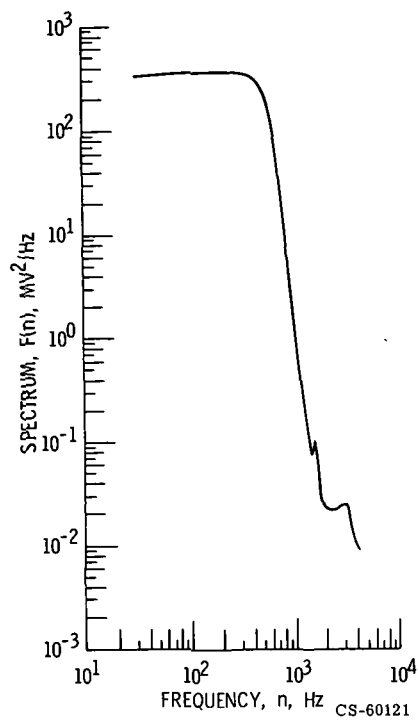


Figure 7

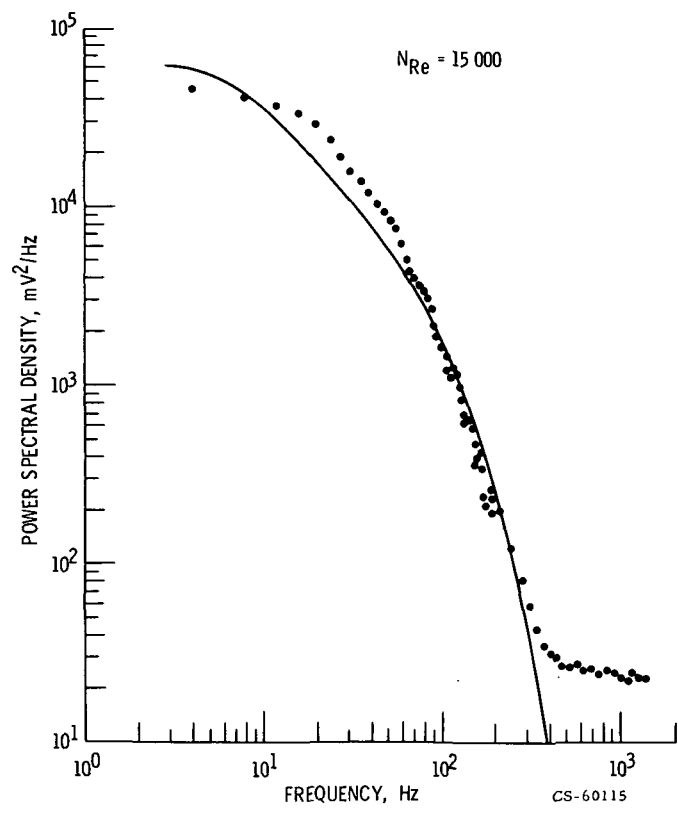


Figure 8

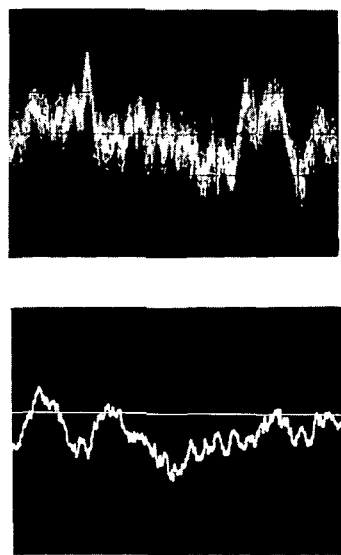


Figure 9

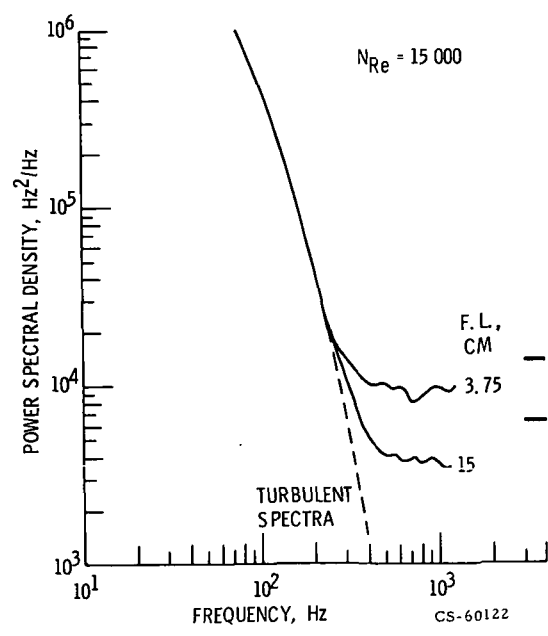


Figure 10

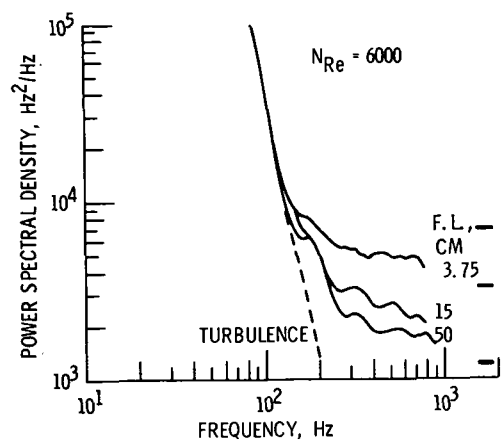


Figure 11

CS-60124

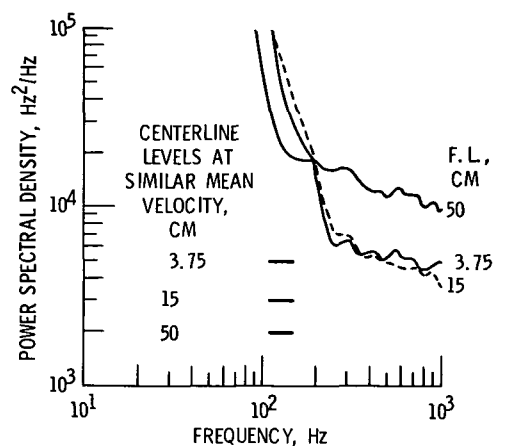


Figure 12

CS-60123

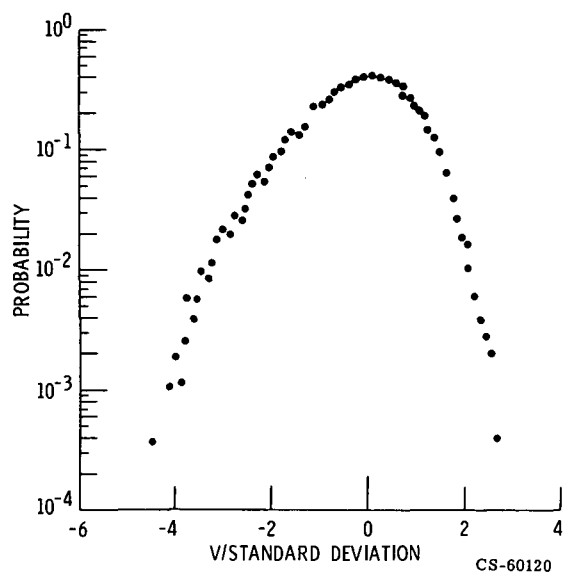


Figure 13

CS-60120

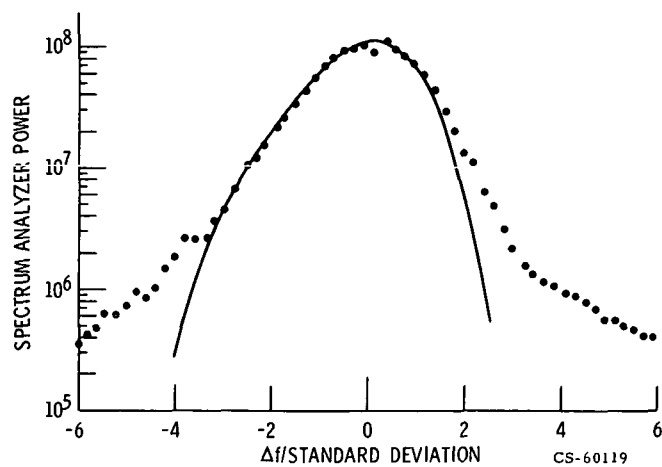


Figure 14

CS-60119

E-6683

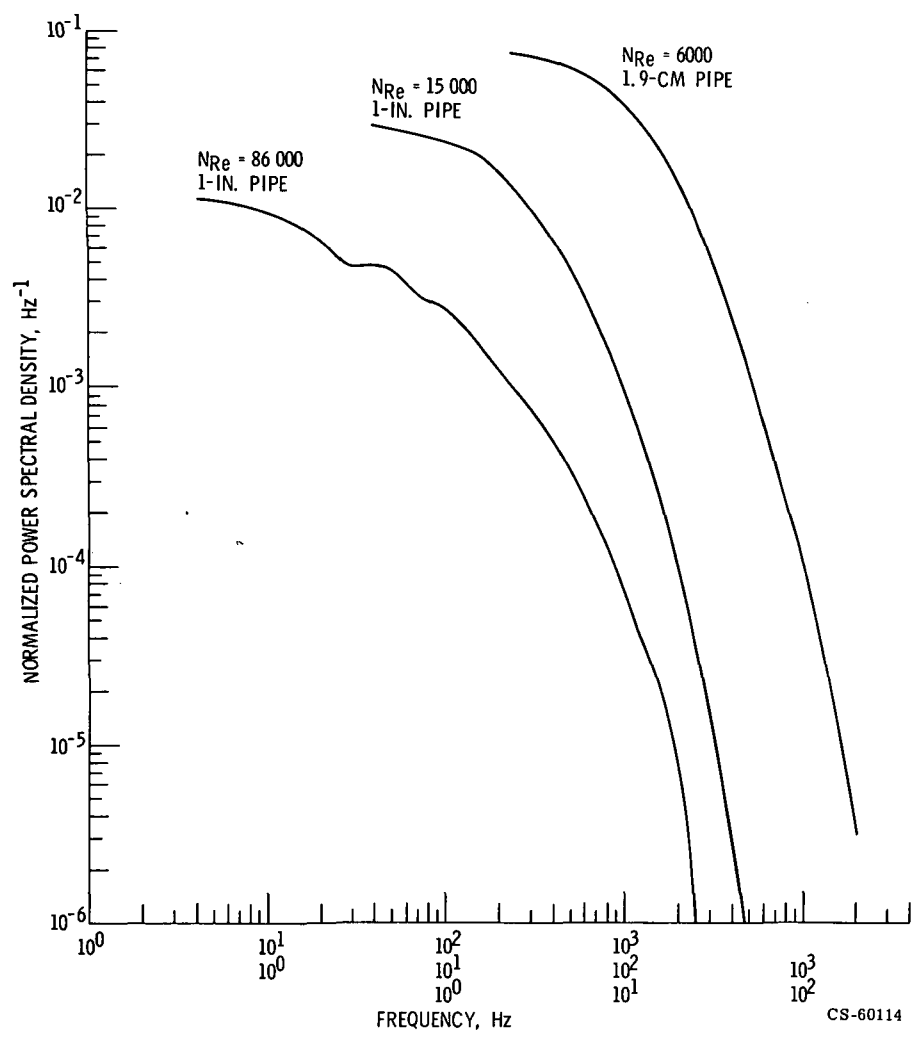


Figure 15

CS-60114